NMR and EPR Spectroscopic and Structural Studies of Low-Spin, $(d_{xz},d_{yz})^4(d_{xy})^1$ Ground State Fe(III) Bis-*tert*-Butylisocyanide Complexes of Dodecasubstituted Porphyrins[†]

Liliya A. Yatsunyk and F. Ann Walker*

Department of Chemistry, University of Arizona, Tucson, Arizona 85721-0041

The bis-(1,1-dimethylethylisocyanide) (*tert*-butylisocyanide) complexes of three iron porphyrinates (2,3,7,8,12,13,17,18-octaethyl-5,10,15,20-tetraphenylporphyrin, OETPP; 2,3,7,8,12,13,17,18-octamethyl-5,10,15,20-tetraphenylporphyrin, OMTPP; and 2,3,7,8,12,13,17,18-tetra-β,β'-tetramethylene-5,10,15,20-tetraphenylporphyrin, TC_6TPP) have been prepared and studied by EPR and ¹H NMR spectroscopy. From EPR and NMR spectroscopic results it has been found that the ground states of the bis-(*t*-BuNC) complexes of OETPP, OMTPP, and TC_6TPP are represented mainly (99.1–99.4%) as $(d_{xz},d_{yz})^4(d_{xy})^1$ electron configurations, with an excited state lying 700 cm^{-1} to higher energy for the OMTPP complex, and probably at lower and higher energies, respectively, for the OETPP and TC_6TPP complexes. In the ¹H NMR spectra the $(d_{xz},d_{yz})^4(d_{xy})^1$ electron configurations of all three complexes are indicated by the large and positive *meso*-phenyl-H shift differences, $\delta_m-\delta_o$ and $\delta_m-\delta_p$, and close to the diamagnetic shifts of groups (CH_3 or CH_2) directly attached to the β-carbons. However, in comparison to *meso*-only substituted porphyrinates such as [FeTPP(*t*-BuNC)$_2$]ClO$_4$, the *meso*-phenyl shift differences are much smaller, especially for the OETPP complex. 2D NOESY spectra show that the flexibility of the porphyrin core decreases with increasing nonplanar distortion in the order TC_6TPP > OMTPP > OETPP and in the same order the stability of the binding to *t*-BuNC ligands decreases. In addition, the structures of two crystalline forms of [FeOMTPP(*t*-BuNC)$_2$]ClO$_4$ have been determined by X-ray crystallography. Both structures showed purely saddled porphyrin cores and somewhat off-axis binding of the isocyanide ligands. To our knowledge, this is the first example of a porphyrin complex with a purely saddled conformation that adopts the $(d_{xz},d_{yz})^4(d_{xy})^1$ ground state. All structurally-characterized complexes of this electron configuration reported previously are ruffled. Therefore, we conclude that a *ruffled geometry stabilizes the $(d_{xz},d_{yz})^4(d_{xy})^1$ ground state, but is not necessary for its existence.*

Introduction

Past investigations of the effects of the σ-donor, π-donor/acceptor properties of axial ligands on the spectroscopic properties and structures of Fe(III) porphyrinates have highlighted the importance of EPR, NMR, MCD, and Mössbauer spectroscopy, as well as molecular structure determination, in delineating the electronic ground state of ferriheme complexes.[1–9] In particular, Mössbauer, EPR, and

NMR studies of the bis-isocyanide complexes[†] of low-spin [FeTPP(*t*-BuNC)$_2$]ClO$_4$ and [FeOEP(*t*-BuNC)$_2$]ClO$_4$,[7] and

* To whom correspondence should be addressed. E-mail: jacs@ u.arizona.edu.

[†] Abbreviations used in this paper are as follows: *t*-BuNC = 1,1-dimethylethylisocyanide; OETPP = 2,3,7,8,12,13,17,18-octaethyl-5,10,15,20-tetraphenylporphyrin; OMTPP = 2,3,7,8,12,13,17,18-octamethyl-5,10,15,20-tetraphenylporphyrin; TC_6TPP = 2,3,7,8,12,13,17,18-tetra-β,β'-tetramethylene-5,10,15,20-tetraphenylporphyrin; T^{n}PrP = *meso*-tetra-*n*-propylporphyrin; T^{i}PrP = *meso*-tetraisopropylporphyrin; T^{c}PrP = *meso*-tetracyclopropylporphyrin.

(1) Walker, F. A.; Huynh, B. H.; Scheidt, W. R.; Osvath, S. R. *J. Am. Chem. Soc.* **1986**, *108*, 5288−5297.
(2) Scheidt, W. R.; Kirner, J. F.; Hoard, J. L.; Reed, C. A. *J. Am. Chem. Soc.* **1987**, *109*, 1963−1968.
(3) Simonneaux, G.; Hindre, F.; Plouzennec, M. L. *Inorg. Chem.* **1989**, *28*, 823−825.
(4) Safo, M. K.; Gupta, G. P.; Walker, F. A.; Scheidt, W. R. *J. Am. Chem. Soc.* **1991**, *113*, 5497−5510.
(5) Safo, M. K.; Gupta, G. P.; Watson, C. T.; Simonis, U.; Walker, F. A.; Scheidt, W. R. *J. Am. Chem. Soc.* **1992**, *114*, 7066−7075.
(6) Safo, M. K.; Walker, F. A.; Raitsimring, A. M.; Walters, W. P.; Dolata, D. P.; Debrunner, P. G.; Scheidt, W. R. *J. Am. Chem. Soc.* **1994**, *116*, 7760−7770.
(7) Walker, F. A.; Nasri, H.; Turowska-Tyrk, I.; Mohanrao, K.; Watson, C. T.; Shokhirev, N. V.; Debrunner, P. G.; Scheidt, W. R. *J. Am. Chem. Soc.* **1996**, *118*, 12109−12118.
(8) Cheesman, M. R.; Walker, F. A. *J. Am. Chem. Soc.* **1996**, *118*, 7373−7380.

the related [FeTTP(2,6-XylylNC)$_2$]ClO$_4$ complex,[9] have shown that their g values ($g_\perp = 2.20-2.28$, $g_{||} = 1.94-1.83$) are consistent with the purest $(d_{xz},d_{yz})^4(d_{xy})^1$ ground state observed so far, with almost complete quenching of orbital momentum ($\Sigma g^2 = 13.5$, substantially smaller than the theoretical value of 16[10]). This pure d_{xy} unpaired electronic state is believed to be due to the *weak σ-donating* and *strong π-accepting* properties of the axial *t*-BuNC ligand and the *ruffled* geometry of the porphyrin cores. Detailed pulsed EPR investigations of [FeTPP(PhNC)$_2$]$^+$ [11] and [*meso*-^{13}C-TPPFe-(*t*-BuNC)$_2$]$^+$ [12] allowed direct determination of the spin density at the *meso*-[12] and axial ligand[11] carbons and confirmed the orientation of the *g*-tensor, with the smallest *g* value aligned along the normal to the heme plane. Thus, the spin density distribution and unpaired electron occupation of the d_{xy} orbital of low-spin Fe(III) are now well established for bis-isocyanide complexes that are highly ruffled.

2,3,7,8,12,13,17,18-Octaethyl-5,10,15,20-tetraphenylporphyrinato iron(III) systems, OETPPFe(III), can be viewed as formula hybrids of TPP and OEP iron(III) porphyrins and therefore would be expected to have the $(d_{xz},d_{yz})^4(d_{xy})^1$ ground state if bound to weak σ-donor, strong π-acceptor axial ligands such as *t*-BuNC. The same can be suggested for other octaalkyltetraphenylporphinatoiron(III) complexes, including OMTPPFe(III) and TC$_6$TPPFe(III). As has been shown for bis-imidazole and bis-pyridine complexes, the degree of nonplanar distortion and saddledness decreases in the order OETPP > OMTPP > TC$_6$TPP, with the latter core having approximately 40% ruffled character.[13] Recent searches of Shelnutt and co-workers have revealed that nonplanar distortion of porphyrins is frequently observed in naturally occurring heme proteins,[14-16] and it has been suggested that such distortions may play an important role in tuning their redox and spectroscopic properties. Therefore, a major question arose as to how the type and degree of deformation of the porphyrin ring might affect the electron configuration. It is already well-known that ruffling of the porphyrin core stabilizes the $(d_{xz},d_{yz})^4(d_{xy})^1$ electronic ground state for Fe(III) porphyrinates by strengthening porphyrin $a_{2u}(\pi)$-metal d_{xy} bonding.[6,7] This interaction is only possible for the ruffled geometry of the porphyrin core, where the twist of pyrrole rings creates a ~15° tilt in the orientation of the porphyrin nitrogen p$_z$ orbitals that produces a projection of these p$_z$ orbitals in the *xy* plane.[6] However, the geometry of saddle-shaped porphyrins does not yield proper N$_P$ p$_z$ orbital

symmetry for overlap with the d_{xy} orbital of Fe(III). The questions then arise as to whether a porphyrin core with a saddled shape can stabilize (and if so, how) the novel $(d_{xz},d_{yz})^4(d_{xy})^1$ ground state, or whether typically saddled porphyrins must adopt a ruffled geometry when bound to π-accepting axial ligands such as *t*-BuNC, to stabilize the $(d_{xz},d_{yz})^4(d_{xy})^1$ ground state of LS Fe(III). The work presented in this paper was carried out in an attempt to answer these questions and was encouraged by the work of Ibers,[17] Simonneaux,[3,9] Nakamura,[18] Scheidt,[7] and our laboratory[7-9] on the properties and structures of various porphyrinato-iron(III) bis-isocyanide complexes. X-ray crystallographic structural data for two crystalline forms of [FeOMTPP(*t*-BuNC)$_2$]ClO$_4$, polycrystalline and frozen solution EPR and variable-temperature 1D and 2D NMR spectroscopic investigations of the low-spin Fe(III) highly distorted complexes of [FeOMTPP(*t*-BuNC)$_2$]ClO$_4$, [FeOETPP(*t*-BuNC)$_2$]ClO$_4$, and [FeTC$_6$TPP(*t*-BuNC)$_2$]ClO$_4$ are presented and discussed in this work.

Experimental Section

Sample Preparation. The three 2,3,7,8,12,13,17,18-octaalkyl-5,10,15,20-tetraphenylporphyrin free bases and their Fe(III) complexes (with chloride counterion) were prepared according to reported procedures,[13] and the chloride anion was exchanged for perchlorate as previously described.[19,20] [*Caution! Perchlorate salts are potentially explosive when heated or shocked. Handle them in milligram quantities with care.*] The NMR sample of [FeOMTPP-(*t*-BuNC)$_2$]ClO$_4$ was prepared by addition of 3−6 equiv of *t*-BuNC to 3 mg of (OMTPP)FeClO$_4$ in 0.3 mL of CD$_2$Cl$_2$ in an NMR sample tube. The color changed immediately from the red-brown of (OMTPP)FeClO$_4$ to a green-brown, indicating formation of [FeOMTPP(*t*-BuNC)$_2$]ClO$_4$. After all NMR experiments were completed, the content of the NMR tube was split into two parts, and the samples were concentrated to 0.1 mL by leaving them open for a day or two. These concentrated CD$_2$Cl$_2$ solutions of [Fe-OMTPP(*t*-BuNC)$_2$]ClO$_4$ were layered carefully with *o*-xylene in one tube and with dodecane in another. The tubes were capped, sealed with Parafilm, and protected from light with aluminum foil. X-ray quality crystals appeared after 7−10 days. [FeOETPP(*t*-BuNC)$_2$]ClO$_4$ and [FeTC$_6$TPP(*t*-BuNC)$_2$]ClO$_4$ NMR samples were prepared in the same manner. Many attempts were made to obtain crystals of those complexes by liquid diffusion methods using the following solvent systems: toluene only, chlorobenzene/dodecane, chloroform/cyclohexane, methylene chloride/*o*-xylene, and methylene chloride/dodecane. However, all attempts were unsuccessful and in the best case (methylene chloride/dodecane) crystals of [FeOETPP(*t*-BuNC)$_2$]ClO$_4$ were obtained that were merohedral twins whose structure solution was never achieved. As for [FeTC$_6$-TPP(*t*-BuNC)$_2$]ClO$_4$, instead of producing crystals or even solids, the sample turned into a dark-brown oil. This was not surprising, as a number of other attempts to get crystals of TC$_6$TPPFe(III) with various pyridine and imidazole ligands were also unsuccessful; only

(9) Simonneaux, G.; Schünemann, V.; Morice, C.; Carel, L.; Toupet, L.; Winkler, H.; Trautwein, A. X.; Walker, F. A. *J. Am. Chem. Soc.* **2000**, *122*, 4366−4377.
(10) Taylor, C. P. S. *Biochim. Biophys. Acta* **1977**, *491*, 137−148.
(11) Astashkin, A. V.; Raitsimring, A. M.; Kennedy, A. R.; Shokhireva, T. Kh.; Walker, F. A. *J. Phys. Chem. A* **2002**, *106*, 74−82.
(12) Rivera, M.; Caignan, G. A.; Astashkin, A. V.; Raitsimring, A. M.; Shokhireva, T. Kh.; Walker, F. A. *J. Am. Chem. Soc.* **2002**, *124*, 6077−6089.
(13) Yatsunyk, L. A.; Carducci, M. D.; Walker, F. A. *J. Am. Chem. Soc.* **2003**, *125*, 15986−16005.
(14) Shelnutt, J. A.; Song, X.-Z.; Ma, J. G.; Jia, S.-L.; Jentzen, W.; Medforth, C. J. *J. Chem. Soc. Rev.* **1998**, *27*, 31−41.
(15) Shelnutt, J. A. *J. Phys. Chem.* **1989**, *93*, 6283−6290.
(16) Ma, J.-G.; Zhang, J.; Franco, R.; Jia, S.-L.; Moura, I.; Moura, J. G.; Kroneck, P. M. H.; Shelnutt, J. A. *Biochemistry* **1998**, *37*, 12431−12442.

(17) Jameson, G. B.; Ibers, J. A. *Inorg. Chem.* **1979**, *18*, 1200−1208.
(18) Ikeue, T.; Ohgo, Yo.; Saitoh, T.; Yamaguchi, T.; Nakamura, M. *Inorg. Chem.* **2001**, *40*, 3423−3434.
(19) Nesset, M. J. M.; Cai, S.; Shokhireva, T. Kh.; Shokhirev, N. V.; Jacobson, S. E.; Jayaraj, K.; Gold, A.; Walker, F. A. *Inorg. Chem.* **2000**, *39*, 532−540.
(20) Yatsunyk, L. A.; Walker, F. A. *Inorg. Chem.* **2004**, *43*, 757−777.

Table 1. Experimental Details and Crystal Data for [FeOMTPP(*t*-BuNC)$_2$]ClO$_4$, Molecules A and B

	Molecule A: [FeOMTPP(*t*-BuNC)$_2$]ClO$_4$·CH$_2$Cl$_2$·1.4C$_{12}$H$_{26}$	Molecule B: [FeOMTPP(*t*-BuNC)$_2$]ClO$_4$·CH$_2$Cl$_2$
empirical formula	FeN$_6$C$_{80}$H$_{99}$O$_4$Cl$_3$	FeN$_6$C$_{63}$H$_{64}$O$_4$Cl$_3$
fw	1370.85	1131.40
T, K	100(2)	170(2)
crystal system	orthorhombic	monoclinic
space group	*Pmna*	*P2$_1$/m*
a, Å	29.311(4)	12.302(6)
b, Å	17.068(2)	17.698(8)
c, Å	14.0209(19)	14.257(7)
β	90°	114.873(5)°
V, Å^3	7014.5(16)	2816(2)
Z	4	2
density (calc), g/cm^3	1.298	1.334
abs coeff, mm^{-1}	0.385	0.464
F(000)	2920	1186
crystal dimension, mm^3	0.36 × 0.25 × 0.06	0.39 × 0.26 × 0.2
θ limits	1.61 to 20.84°	1.82 to 25.64°
limiting indices	$-29 \leq h \leq 29, -17 \leq k \leq 17, -14 \leq l \leq 14$	$-14 \leq h \leq 14, -21 \leq k \leq 21, -17 \leq l \leq 17$
reflns utilized	43978	25342
independent reflns	3834 [R$_{int}$ = 0.1344]	5481 [R$_{int}$ = 0.1570]
completeness, %	99.8	99.4
absorption correction	none	Psi-scan
max./min. transmission	0.9773/0.8738	0.9464/0.8397
data/restraints/parameters	3834/10/475	5481/0/374
GoF on F^2	1.061	0.877
Final R indices [$I > 2\sigma(I)$]	R$_1$ = 0.0637, wR$_2$ = 0.1504	R$_1$ = 0.0535, wR$_2$ = 0.0912
R indices (all data)	R$_1$ = 0.1413, wR$_2$ = 0.2041	R$_1$ = 0.1206, wR$_2$ = 0.1042
largest diff. peak and hole	0.634 and -0.524 e/Å^3	0.460 and -0.392 e/Å^3
RMS difference density	0.079 e/Å^3	0.058 e/Å^3

[FeTC$_6$TPP(1-MeIm)$_2$]Cl was successfully crystallized and the structure solved.[13]

Spectroscopy. EPR spectra were recorded on a Bruker ESP-300E spectrometer (operating at 9.4 GHz with 100 kHz field modulation) equipped with an Oxford Instruments ESR 900 continuous flow helium cryostat, at 4.2 K. Spectra were obtained for samples in frozen CD$_2$Cl$_2$ solutions and as crystalline samples.

^{1}H NMR spectra were acquired using a Varian Unity-300 spectrometer operating at 299.957 MHz and equipped with a broad-band inverse probe and variable-temperature controller in CD$_2$Cl$_2$ in the temperature range from +30 to -93 °C. 2D spectra (COSY, DQF$-$COSY, NOESY, and ROESY) were acquired at a number of temperatures between 20 and -90 °C using the standard pulse sequences. Data were acquired with 512 complex pairs in the directly detected dimension and 128 t$_1$ increments. The relaxation delay was set to the average T_1 of the protons that are the closest to the paramagnetic center (phenyl-*o*, bound ligand, and methylene protons in OETPP and TC$_6$TPP, and methyl protons in OMTPP). The relaxation time delay in 2D experiments was set so that the total recycling time was longer than or equal to the longest T_1. The processing parameters are described in detail in the caption for Figure 5. T_1 data were acquired using standard T_1 inversion$-$recovery pulse sequences. In NOESY spectra the peak volumes for kinetic studies were measured using the standard Varian VNMR and Felix software. Fitting of the data for the Curie plots was done using the 2-level temperature-dependent fitting program created by Dr. Nikolai Shokhirev in this laboratory.[21,22]

Structure Determination: General. Two crystalline forms of [FeOMTPP(*t*-BuNC)$_2$]ClO$_4$ grown from CD$_2$Cl$_2$/dodecane (denoted as molecule A) and CD$_2$Cl$_2$/*o*-xylene (molecule B) were mounted on glass fibers in random orientations and examined on a Bruker

SMART 1000 CCD detector X-ray diffractometer at 100(2) K and 170(2) K, respectively. All measurements utilized graphite mono-chromated Mo Kα radiation ($\lambda = 0.71073$ Å) with a power setting of 50 kV, 40 mA. Final cell constants and complete details of the intensity collection and least squares refinement parameters are summarized in Table 1.

In both cases, a total of 3736 frames at one detector setting covering $0 < 2\theta < 60°$ were collected, having an omega scan width of 0.2° and 0.3° and an exposure time of 20 s per frame for A and B, respectively. The frames were integrated using the Bruker SAINT software package's narrow frame algorithm.[23] Initial cell constants and an orientation matrix for integration were determined from reflections obtained in three orthogonal 5° wedges of reciprocal space.

Both structures were solved using SHELXS in the Bruker SHELXTL (Version 6.0) software package.[24] The crystals of A were nonmerohedral twins with one fragment much larger than the other. The data for the major component only were integrated. Details of the structure solution and refinement are described in the Supporting Information. Refinements were performed using SHELXL and illustrations were made using XP.[24] Solution was achieved utilizing direct methods followed by Fourier synthesis. Hydrogen atoms were added at idealized positions, constrained to ride on the atom to which they are bonded, and given thermal parameters equal to 1.2 or 1.5 times U_{iso} of that bonded atom. Scattering factors and anomalous dispersion were taken from the International Tables (Vol. C Tables 4.2.6.8 and 6.1.1.4).

Tables of final fractional atomic coordinates and anisotropic thermal parameters for the non-hydrogen atoms in [FeOMTPP(*t*-BuNC)$_2$]ClO$_4$ (A and B) are listed in the Supporting Information Figures S1$-$S10.

(21) Shokhirev, N. V.; Walker, F. A. *J. Phys. Chem.* **1995**, *99*, 17795$-$17804.
(22) http://www.shokhirev.com/nikolai/programs/prgsciedu.html.
(23) *Bruker 2002 SAINT Reference Manual, Version 6.0*; Bruker AXS Inc.: Madison, WI, 2002.
(24) *Bruker 2002 SHELXTL Reference Manual, Version 6.0*; Bruker AXS Inc.: Madison, WI, 2002.

Table 2. EPR Data for [FeOETPP(*t*-BuNC)$_2$]ClO$_4$, [FeOMTPP(*t*-BuNC)$_2$]ClO$_4$, and [FeTC$_6$TPP(*t*-BuNC)$_2$]ClO$_4$

parameter	[FeOETPP(*t*-BuNC)$_2$]$^+$	[FeOMTPP(*t*-BuNC)$_2$]$^+$	[FeTC$_6$TPP(*t*-BuNC)$_2$]$^+$
$g_\perp$	2.235	2.192	2.199
$g_\parallel$	1.928	1.942	1.939
Σg^2	13.707	13.380	13.388
V/λ^a	0.000	0.000	0.000
Δ/λ^a	−7.712	−9.211	−8.552
V/Δ^a	0.000	0.000	0.000
a, b	0.068	0.057	0.061
c	0.991	0.992	0.989
$a^2 + b^2 + c^2$	0.992	0.990	0.986
k^b	1.008	1.010	1.014
%d_{xy} ^{c}	99.1	99.4	99.3

^{a} All crystal field parameters were calculated assuming Taylor's "proper axis system",[10] with $g_y = -g_x = g_\perp$, and $g_z = -g_\parallel$. ^{b} k is the orbital reduction parameter defined as $1/(a^2 + b^2 + c^2)$. ^{c} The effective %d_{xy} character was calculated as kc^2.
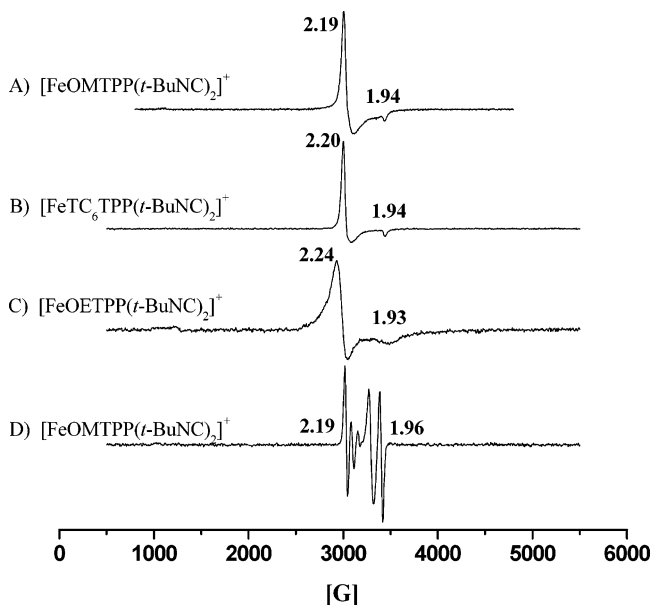

Figure 1. (A−C) Frozen solution EPR spectra of [FeOMTPP(*t*-BuNC)$_2$]-ClO$_4$, [FeOETPP(*t*-BuNC)$_2$]ClO$_4$, and [FeTC$_6$TPP(*t*-BuNC)$_2$]ClO$_4$ at 4.2 K in CD$_2$Cl$_2$, respectively. All three EPR spectra are very similar and are of the axial type that is characteristic of the $(d_{xz},d_{yz})^4(d_{xy})^1$ ground state. (D) 4.2 K EPR spectrum of a polycrystalline sample of [FeOMTPP(*t*-BuNC)$_2$]ClO$_4$ obtained by crystallization from toluene.

Results and Discussion

EPR Spectroscopy. The EPR spectra of [FeOMTPP(*t*-BuNC)$_2$]ClO$_4$, [FeOETPP(*t*-BuNC)$_2$]ClO$_4$, and [FeTC$_6$TPP-(*t*-BuNC)$_2$]ClO$_4$ were measured at 4.2 K in frozen solutions of CD$_2$Cl$_2$, and are shown in Figure 1A−C. These complexes exhibit axial EPR spectra with $g_\perp = 2.19$, $g_\parallel = 1.94$, $g_\perp = 2.24$, $g_\parallel = 1.93$, and $g_\perp = 2.20$, $g_\parallel = 1.94$ for [FeOMTPP-(*t*-BuNC)$_2$]ClO$_4$, [FeOETPP(*t*-BuNC)$_2$]ClO$_4$, and [FeTC$_6$-TPP(*t*-BuNC)$_2$]ClO$_4$, respectively. In addition, the EPR spectra of polycrystalline [FeOMTPP(*t*-BuNC)$_2$]ClO$_4$ from toluene at different rotation angles were obtained, and one of them is presented in Figure 1D. Because of the presence of multiple orientations of porphyrin molecules in the crystals these spectra contain numerous signals, but all of them are in the range from 2.19 to 1.96, which is consistent with the limits expected for the axial type of EPR signal in frozen CD$_2$Cl$_2$ solution of [FeOMTPP(*t*-BuNC)$_2$]ClO$_4$. It was impossible to solve the crystal structure for this sample because the crystals were of poor quality and did not diffract well. Nakamura et al.[18] have reported a very similar EPR

spectrum for [FeOETPP(*t*-BuNC)$_2$]ClO$_4$ and a much broader spectrum for [FeOMTPP(*t*-BuNC)$_2$]ClO$_4$ with almost unre-solved $g_\parallel$. Both EPR spectra of that work were viewed as rhombic with similar g_2 and g_3 values, and were fit with three g values $g_3 = 2.20$, $g_2 = 2.17$, $g_1 = 1.95$; and $g_3 = 2.29$, $g_2 = 2.25$, $g_1 = 1.92$, for OETPP and OMTPP respec-tively.[18] The EPR spectrum that we observe for [FeOMTPP-(*t*-BuNC)$_2$]ClO$_4$ in frozen CD$_2$Cl$_2$ solution is much sharper, with clearly resolved $g_\perp = 2.19$, $g_\parallel = 1.94$ (Figure 1A). Axial EPR spectra with very similar g values have been obtained for other bis-isocyanide Fe(III) porphyrinates: [FeTPP(*t*-BuNC)$_2$]ClO$_4$ ($g_\perp = 2.21$, $g_\parallel = 1.93$),[7,18] [FeOEP(*t*-BuNC)$_2$]-ClO$_4$ ($g_\perp = 2.28$, $g_\parallel = 1.83$),[7,18] [FeProtoIXMe$_2$(*t*-BuNC)$_2$]-ClO$_4$ ($g_\perp = 2.30$, $g_\parallel = 1.86$[18]), and bis-(*t*-BuNC) complexes of T^{i}PrP, T^{c}PrP, and T^{n}PrP ($g_\perp = 2.16$, $g_\parallel = 1.95$[18]), as well as for [FeTTP(2,6-XylylNC)$_2$]ClO$_4$ ($g_\perp = 2.15$, $g_\parallel = 1.94$[9]).

The crystal field parameters for the three bis-(*t*-BuNC) complexes, of OMTPP, OETPP, and TC$_6$TPP, presented in Table 2, were calculated following the procedure described by Simonneaux et al.[9] They indicate a very pure $(d_{xz},d_{yz})^4(d_{xy})^1$ ground state with ∼99% d_{xy} character and little spin−orbit mixing with the d_{xz} and d_{yz} orbitals (a and b coefficients are very small) for all three porphyrin complexes of this study. The rhombic splitting, V/λ, is 0.0 due to the degeneracy of the d_{xz} and d_{yz} orbitals; the negative sign of the tetragonality parameter, Δ/λ, indicates that the d_{xy} orbital is above the d_{xz} and d_{yz} orbitals, and the absolute values of Δ/λ of 7.71, 8.52, and 9.21λ indicate the gap between d_{xy} and d_π orbitals of low-spin Fe(III) in [FeOMTPP(*t*-BuNC)$_2$]ClO$_4$, [FeTC$_6$TPP-(*t*-BuNC)$_2$]ClO$_4$, and [FeOETPP(*t*-BuNC)$_2$]ClO$_4$, respec-tively. The large deviation of the Σg^2 from the ideal value of 16 (Table 2) indicates that a substantial amount of orbital angular momentum is quenched, yet the g values clearly identify the unpaired electron as occupying a predominately metal d rather than a porphyrin π molecular orbital composed of C and N p$_z$ orbitals. Very similar crystal field parameters were obtained for [FeTPP(*t*-BuNC)$_2$]ClO$_4$ and [FeOEP(*t*-BuNC)$_2$]ClO$_4$.[7] The tetragonality, Δ/λ, of bis-(4-CNPy) iron-(III) porphyrin complexes is substantially lower,[6,20] indicating poorer σ-donating properties of 4-CNPy ligand as compared to *t*-BuNC.

Structures of [FeOMTPP(*t*-BuNC)$_2$] ClO$_4$ (from CD$_2$Cl$_2$/ Dodecane, Molecule A, and CD$_2$Cl$_2$/*o*-Xylene, Molecule B). The molecular structure of [FeOMTPP(*t*-BuNC)$_2$]ClO$_4$,

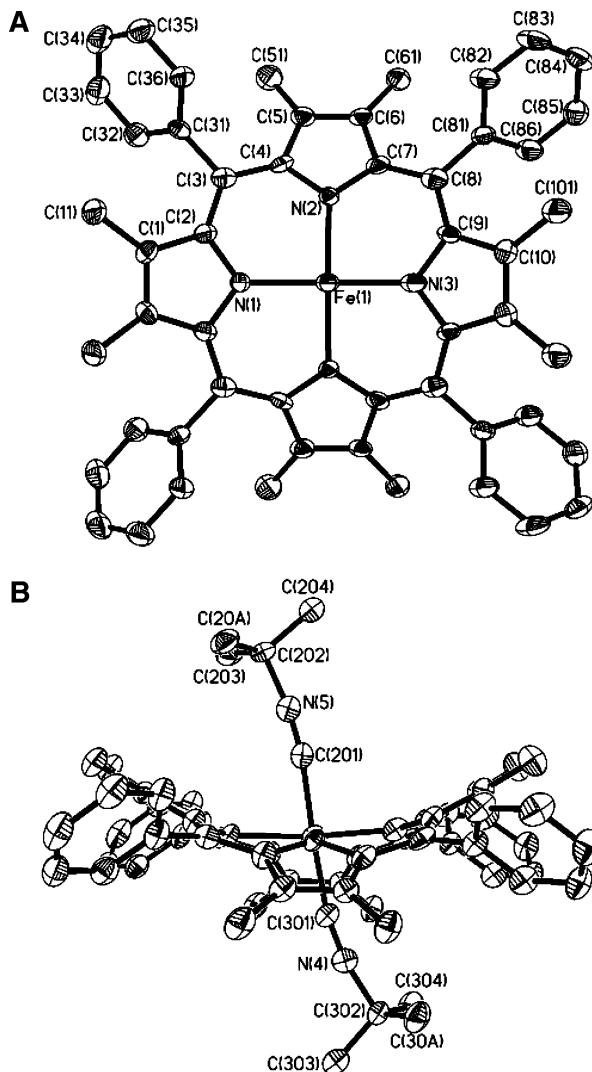**Figure 2.** (A) ORTEP diagram and atom labels for the porphyrin macrocycle of [FeOMTPP(*t*-BuNC)₂]ClO₄, molecule A. The mirror plane lies along the N1−Fe−N3 axis perpendicular to the porphyrin mean plane. (B) Edge-on view and numbering scheme for the axial ligands. The porphyrin core is purely saddled. Thermal ellipsoids enclose 50% probability, and hydrogens are omitted for clarity.
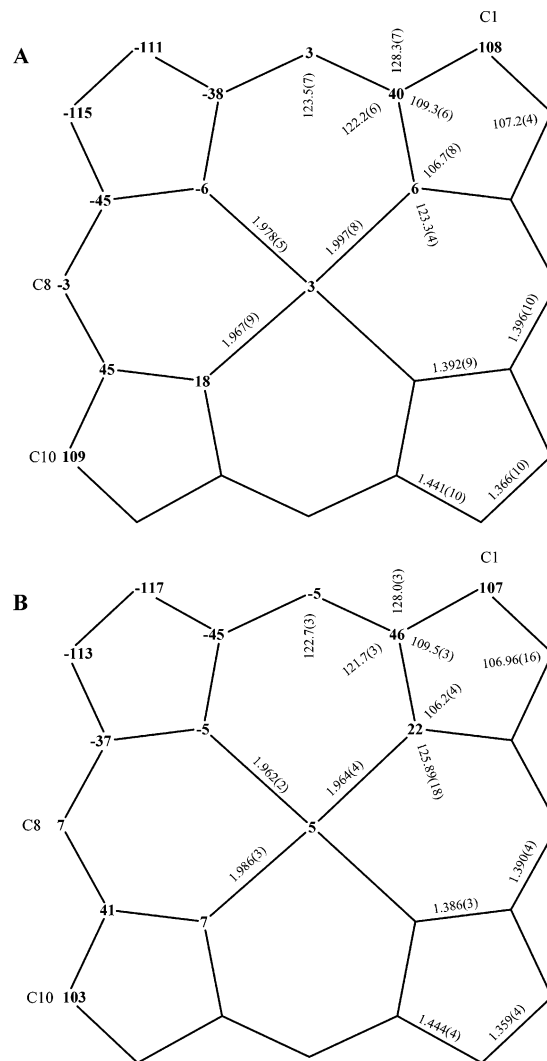

Figure 3. Formal diagram of the porphyrinate core in [FeOMTPP(*t*-BuNC)₂]⁺ for molecules A and B, showing the displacement of the atoms in units of 0.01 Å, from the mean plane of the 25-atom porphyrin core.

molecule A, is shown in the ORTEP diagram (Figure 2) along with the numbering scheme for the crystallographically unique atoms, which reflects the presence of the mirror plane along the N1−Fe−N3 vector. Molecule B has the same basic features and numbering scheme. The deviation of porphyrin cores from planarity was plotted in Figure 3A and B as formal diagrams and in supporting Figure S2 as linear representations in order to obtain a quantitative estimation of the degree and type of nonplanar distortion. The unique feature of both [FeOMTPP(*t*-BuNC)₂]ClO₄ structures is their *strongly saddled porphyrin* core. Nevertheless, NMR (see below) and EPR spectroscopic results both clearly indicate a pure $(d_{xz},d_{yz})^4(d_{xy})^1$ electronic ground state. To our knowledge this is the first structurally characterized molecule where the $(d_{xz},d_{yz})^4(d_{xy})^1$ ground state is stabilized in the presence of a saddled porphyrin core, with no evidence of ruffling, although the OMTPP core can ruffle and a substantial degree of ruffling is observed in the crystal structures of [FeOMTPP-(4-CNPy)₂]ClO₄, 17%,[20] and [FeOMTPP(4-Me₂NPy)₂]Cl,

30%.[13] Other structurally characterized bis-isocyanide complexes of OEP and TPPs adopt almost pure S₄-ruffled conformations.[7,9]

On the basis of 1D ¹H and ¹³C NMR and EPR spectroscopic results for [FeOMTPP(*t*-BuNC)₂]ClO₄ and [FeOETPP(*t*-BuNC)₂]ClO₄, Nakamura and co-workers[18] have predicted for both complexes saddled structures with ruffled deformation, larger in the former complex. At the beginning, we believed that the $(d_{xz},d_{yz})^4(d_{xy})^1$ ground state should be stabilized by both π-accepting axial ligands and ruffled conformation of the porphyrin core, because extreme ruffling of the porphyrinate ring facilitates extensive delocalization of the d_{xy} unpaired electron into the porphyrinate $3a_{2u}(\pi)$ orbital. After obtaining the first saddled structure of [FeOMTPP(*t*-BuNC)₂]ClO₄, molecule A, we hypothesized that although this complex is saddled, it might also be possible to crystallize a form having some ruffling component, in line with the expectation that ruffling should be required for spin delocalization to the porphyrinate core. To test this hypothesis the crystal structures of bis-(*t*-BuNC) complexes of OETP-PFe(III) or TC₆TPPFe(III) or the crystals of [FeOMTPP(*t*-

BuNC)$_2$]ClO$_4$ from different solvent systems were needed. The only successful attempt resulted in crystals of [FeOMT-PP(*t*-BuNC)$_2$]ClO$_4$, molecule B, that again showed an almost purely saddled conformation. In fact, the porphyrin cores of the two structures are remarkably similar (see supporting Figure S2).

The average deviation of the β-Cs from the mean porphyrin plane is ± 1.1 Å for both [FeOMTPP(*t*-BuNC)$_2$]ClO$_4$ molecules. The *meso*-Cs are almost in the porphyrin mean plane (the deviation is only ± 0.03 and ± 0.06 Å for A and B, respectively, indicating a very small degree of ruffling in each case, but slightly more for B than A). The average Fe–N$_P$ bond distance in A, 1.981(7) Å, is typical for other OMTPP complexes with various axial ligands,[18] and longer compared to the same distance in ruffled porphyrins.[4,6,7,9] The average Fe–N$_P$ bond distance in B is only 1.968(3) Å and is 0.013 Å shorter than the same distance in molecule A. Slight ruffling of molecule B compared to A can account for some shortening of the Fe–N$_P$ bond length of molecule B.

The lack of ideal geometry around the Fe(III) atom in [FeOMTPP(*t*-BuNC)$_2$]ClO$_4$ is evident from Figure 2B. The axial ligands are not exactly perpendicular to the mean porphyrin plane, but rather are tilted, forming C$_{ax}$–Fe–N$_P$ angles between 81 and 100° in both molecules. It is interesting to note that the axial ligands are tilted in opposite directions, making the C$_{ax}$–Fe–C$_{ax}$′ (C201–Fe1–C301) angle very close to linear (178° for molecule A and 179° for molecule B). The Fe–C$_{ax}$–N$_{ax}$ groups are also not quite linear (the angles are around 170° for both complexes). Off-axis ligand binding was also seen in [FeOEP(*t*-BuNC)$_2$]$^+$ and [FeTPP(*t*-BuNC)$_2$]$^+$.[7] However, in these complexes both axial ligands were tilted in the same direction producing smaller C$_{ax}$–Fe–C$_{ax}$′ angles of ~174°.[7] The Fe–C$_{ax}$ distances in [FeOMTPP(*t*-BuNC)$_2$]ClO$_4$ differ significantly for the two ligands: 1.909(12) and 1.947(13) Å for C301 and C201, respectively, in the structure of molecule A; and 1.932(5) and 1.965(5) Å, for C301 and C201, respectively, for the structure of B. On average, the Fe–C$_{ax}$ distances are significantly longer in molecule B, and are comparable to the Fe–C$_{ax}$ distances in OEP and TPP.[7]

In summary, both crystalline forms of [FeOMTPP(*t*-BuNC)$_2$]ClO$_4$, obtained from CD$_2$Cl$_2$/dodecane (molecule A) and CD$_2$Cl$_2$/*o*-xylene (molecule B) have similar geometries, with purely saddled porphyrin cores, the most important feature of the structures. An unsymmetrical environment about the iron atoms and tilted axial ligands are also observed.

NMR Studies. Detailed investigation of the ^{1}H and ^{13}C NMR spectra and determination of the degree of spin delocalization in the Fe(III) complexes of OETPP, OMTPP, and various *meso*-tetraalkylporphyrins (T^{n}PrP, T^{i}PrP, and T^{c}PrP) with π-accepting axial ligands has been reported earlier.[18] In the present study, extensive 1D and 2D NMR investigation of correlations between the chemical shifts and electronic properties of bis-(*t*-BuNC) Fe(III) complexes of OMTPP, OETPP, and TC$_6$TPP have been carried out. No 2D NMR data have been reported previous to this study.
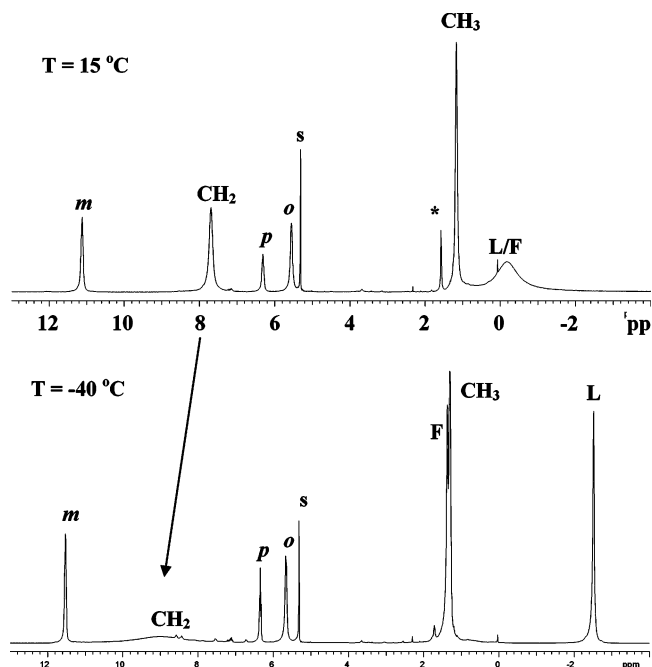
Figure 4. ^{1}H NMR spectra of [FeOETPP(*t*-BuNC)$_2$]ClO$_4$ in CD$_2$Cl$_2$ recorded at 15 and −40 °C, together with peak assignment: *o, m, p*, phenyl resonances; F and L, free and bound ligand *t*-Bu protons; CH$_2$(out) and CH$_2$(in), outer and inner methylene protons; CH$_3$, methyl group of ethyl substituents on the β-Cs; s, solvent, and *, impurities.
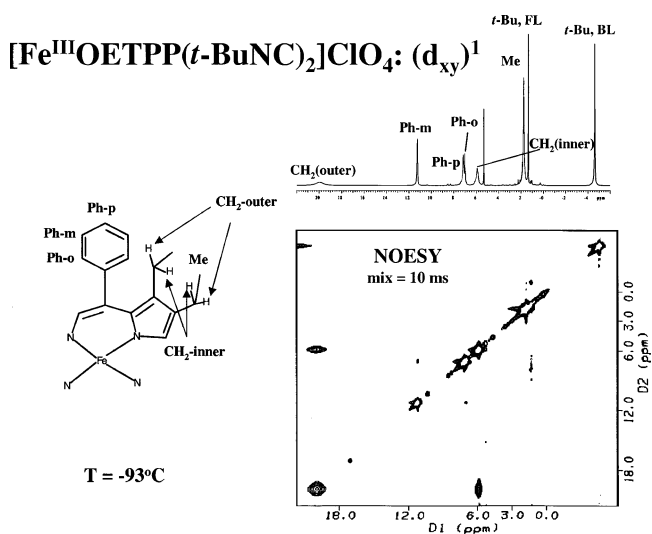

Figure 5. ^{1}H 1D and corresponding 2D NOESY/EXSY NMR spectra for [FeOETPP(*t*-BuNC)$_2$]ClO$_4$ in CD$_2$Cl$_2$ at −93 °C. The NOESY spectrum was acquired with a spectral bandwidth of 8.405 kHz, 512 × 128 complex points, 32 transients per t_1 increment, 10 ms mixing time, and 125 ms relaxation delay between increments. The spectrum was processed in Felix after application of a Gaussian apodization (32 ms and 8 ms). Note the large CE cross-peak between CH$_2$(in) and CH$_2$(out) even at such a low temperature. The insert defines the methylene protons, CH$_2$(in) and CH$_2$(out).

Proton 1- and 2D NMR studies of [FeOETPP(*t*-BuNC)$_2$]-ClO$_4$. Examples of ^{1}H NMR spectra for [FeOETPP(*t*-BuNC)$_2$]ClO$_4$ at 15, −40, and −93 °C are shown in Figures 4 and 5. In addition to porphyrin ethyl and phenyl resonances, free (F) and ligated (L) *t*-BuNC resonances are seen. Peak assignment was based on DQF–COSY and NOESY results, integration of 1D spectra, and values of the relaxation times, T_1s. Chemical shifts and relaxation times for −20 and −90 °C are presented in Table 3. Temperature dependence of the

Table 3. Chemical Shifts and T_1 Relaxation Times for [FeOETPP(t-BuNC)$_2$]ClO$_4$ in CD$_2$Cl$_2$ at Two Temperatures

	$T = -20$ °C		$T = -90$ °C		
peak	shift, ppm	T_1, sec	shift, ppm	T_1, sec	assignment
L	−2.11	0.198(2)	−4.41	0.0623(1)	bound ligand, t-Bu
F	1.37	too broad	1.36	0.810(3)	free ligand, t-Bu
CH$_3$	1.24	0.110(1)	1.72	0.0552(1)	porphyrin methyl
CH$_2$(in)	n/a	n/a	5.83	0.0513(5)	methylene inner
o	5.54	0.0619(3)	6.96	<0.0374(2)[b]	porphyrin *ortho*-phenyl
p	6.30	0.0.357(3)	6.94	<0.244(4)[b]	porphyrin *para*-phenyl
m	11.41	0.292(1)	11.31	0.196(1)	porphyrin *meta*-phenyl
CH$_2$(out)	n/a	n/a	19.42	0.0485(7)	methylene outer
CH$_2$ (av.)[a]	8.33	0.0679(2)	n/a	n/a	methylene outer/inner[a]

[a] Above the coalescence temperature (−55 °C) there is only one methylene peak that is the average between CH$_2$(in) and CH$_2$(out), due to the high rate of ring inversion. As the temperature is lowered, ring inversion slows down and two different chemical environments are detected. [b] At −90 °C phenyl-*ortho* and -*para* resonances are almost overlapped, precluding accurate measurement of T_1. Therefore, reported for these groups are the values of T_1 at −80 °C. Because T_1 decreases as the temperature is lowered we expect phenyl-*ortho* and -*para* protons to have shorter T_1s at −90 °C.

chemical shifts is displayed as a Curie plot in supporting Figure S3. Binding of t-BuNC is relatively unfavorable at any temperature above −20 °C, and an averaged signal for free and bound t-Bu resonances can be seen in the 1D spectra (Figure 4, at 15 °C). However, upon lowering the temperature, this signal broadens and splits into free (F) and bound (L) t-BuNC peaks (Figure 4, at −40 °C). Measurements of spin−lattice relaxation times, T_1, were done at all temperatures. Overall relaxation times for [FeOETPP(t-BuNC)$_2$]-ClO$_4$ are much longer than those for either the OMTPP or TC$_6$TPP analogues (see Tables 3, 4, and 5) due to the lower flexibility of the OETPP complex. T_1 decreases linearly with decreasing temperature for all protons except the free ligand, for which it increases with decreasing temperature (increasing solvent viscosity).

From the simple Curie plot (Figure S3) one can see that, as with most porphyrins containing β-ethyl groups,[25] the methylene signals observed at temperatures below coalescence show curved temperature dependence with intercepts being very different from the diamagnetic shifts of the CH$_2$ protons due to hindered rotation of the ethyl groups at low temperatures; in the case of [FeOETPP(t-BuNC)$_2$]ClO$_4$, the phenyl-H resonances also exhibit somewhat curved temperature dependence. It can be fairly well described by two different linear fits, one for relatively high temperature (from −20 when t-BuNC binds relatively strongly to −55 °C, the coalescence temperature for the methylene peaks) and the other for relatively low temperatures (where the axial ligands are exchanging very slowly with free ligand and chemical exchange due to porphyrin ring inversion is slow on the NMR time scale). Because of hindered rotation of the ethyl groups at lower temperatures, no attempt has been made to analyze in detail the temperature dependence of the chemical shifts for this complex.

In general, there are two different chemical exchange processes that occur in solutions of nonplanar porphyrinates: *ring inversion* and *ligand exchange* (ligand dissociation from the complex and binding of free t-BuCN to the metal). In the case of OETPP there is the additional chemical exchange process that involves rotation of each ethyl group about the CH$_2$−β-pyrrole carbon bond, as

mentioned above, but this is a fairly fast process compared to the others. *Ligand exchange* can be detected in 1D experiments only by the presence of broad lines for free and ligated t-Bu signals. However, a semiquantitative method for studying the ligand exchange process is provided by 2D experiments, NOESY and ROESY, in which two types of cross-peaks can be detected: NOE and chemical exchange. NOE cross-peaks are only 5−10% of the volume of diagonal peaks, due to the inefficiency of magnetization transfer, and are of opposite phase to the diagonal peaks at relatively high temperatures (above ∼ −50 °C), but of the same phase as the diagonal peaks at very low temperatures.[26] In ROESY experiments NOEs are always of negative phase. CE cross-peaks are always in phase with the diagonal peaks and have volumes that depend on the rate of chemical exchange. For [FeOETPP(t-BuNC)$_2$]ClO$_4$, CE cross-peaks are observed between free and bound t-BuNC resonances at all temperatures above −70 °C, until, finally, below −70 °C the ligand exchange process becomes too slow to be detected by NMR spectroscopy. These results contradict the conclusion of Nakamura that the ligand exchange process is frozen below −40 °C,[18] and emphasize the importance of 2D NMR techniques for understanding the dynamics of metalloporphyrin complexes.

The second important chemical exchange process in solutions of nonplanar porphyrins is *ring inversion*. NMR spectroscopy is an excellent tool for obtaining quantitative information about the kinetics of this process. The methylene protons in [FeOETPP(t-BuNC)$_2$]ClO$_4$ appear as a single peak with increasing width as temperature is lowered from 25 to −55 °C (Figure 4). When the temperature is lowered even further, this peak splits into two: CH$_2$(out) due to the diastereotopic methylene protons that point away from each other and toward the phenyl rings; and CH$_2$(in) due to the protons that point toward each other (see scheme in the insert of Figure 5). Unfortunately, no NOE cross-peaks have been detected between CH$_2$(out) and phenyl-*ortho*, which would make the assignment unambiguous, and thus the assignment was made by comparing the chemical shifts of the methylene peaks in [FeOETPP(t-BuCN)$_2$]ClO$_4$ to those in

(25) Isaac, M. F.; Lin, Q.; Simonis, U.; Suffian, D. J.; Wilson, D. L.; Walker, F. A. *Inorg. Chem.* **1993**, *32*, 4030−4041.

(26) Neuhaus, D.; Williamson, M. *The Nuclear Overhauser Effect in Structural and Conformational Analysis*; VCH Publishers: New York, 1989.

[FeOETPP(1-MeIm)$_2$]Cl,[27] [FeOETPP(4-Me$_2$NPy)$_2$]Cl,[27] and [FeOETPP(4-CNPy)$_2$]ClO$_4$,[20,28] for which those NOEs between phenyl and CH$_2$(out) protons were observed. From low temperature 1D ^{1}H NMR studies, the coalescence point, T_c, for the methylene signals in [FeOETPP(t-BuNC)$_2$]ClO$_4$ was found to be -55 °C, which allowed the study of the ring inversion of this complex by both DNMR (above T_c) and 2D NOESY/EXSY techniques (below T_c).[29] From 2D NOESY data at -93 °C shown in Figure 5 it is obvious that the rate of ring inversion is still relatively fast, as strong cross-peaks between CH$_2$(in) and CH$_2$(out) are detected. There is an NOE contribution, of the same sign, to the intensity of these cross-peaks, due to the close proximity of CH$_2$(in) and CH$_2$(out), but the observed intensity is much too high to be accounted for by the NOE alone. We estimate, based upon the intensity of the cross-peaks for [FeOETPP-(4-CNPy)$_2$]ClO$_4$ at -93 °C (3.7% of the intensity of each diagonal peak),[20,33] where chemical exchange had already slowed to the point that it could no longer be observed by NOESY/EXSY techniques, that the contribution of the NOE to the intensity of the cross-peaks shown in Figure 5 is not greater than 5%, and cannot be greater than 10% for any complex at this temperature, whereas the observed cross-peak intensity is roughly 60% that of the diagonal peak when the mixing time is 10 ms; the measured rate of ring inversion from these data is $\sim$50 s^{-1}, as discussed more fully elsewhere.[29,33] Again, this contradicts the claim that the ring inversion process is frozen on the ^{1}H NMR time scale at any temperature below -80 °C judging from 1D spectra only.[28] Direct comparison is possible in this case because both we and previous workers[28] used the same magnetic field strength, 7.2 T (300 MHz for ^{1}H). Detailed analysis of the kinetics data for ring inversion in [FeOETPP(t-BuNC)$_2$]ClO$_4$ and a number of other Fe(III) complexes of the three 2,3,7,8,12,13,17,18-octaalkyl-5,10,15,20-tetraphenylporphyrins of this study are discussed elsewhere.[29,33]

Proton 1- and 2D NMR studies of [FeOMTPP(t-BuNC)$_2$]ClO$_4$. Example ^{1}H NMR spectra of [FeOMTPP(t-BuNC)$_2$]ClO$_4$ at -10 and -90 °C are shown in supporting Figure S4. The Curie plot of the data obtained over the temperature range 179−293 K is shown in Figure 6; peak assignments, together with the T_1 relaxation times of the protons of interest, are presented in Table 4. In the Curie plot, all resonances except the porphyrin CH$_3$ have linear temperature dependence with close to diamagnetic intercepts at $T^{-1} = 0$. The nondiamagnetic intercept of the β-CH$_3$ group is an indication of the existence of a thermally accessible excited state for this complex.[21] Analysis of the temperature
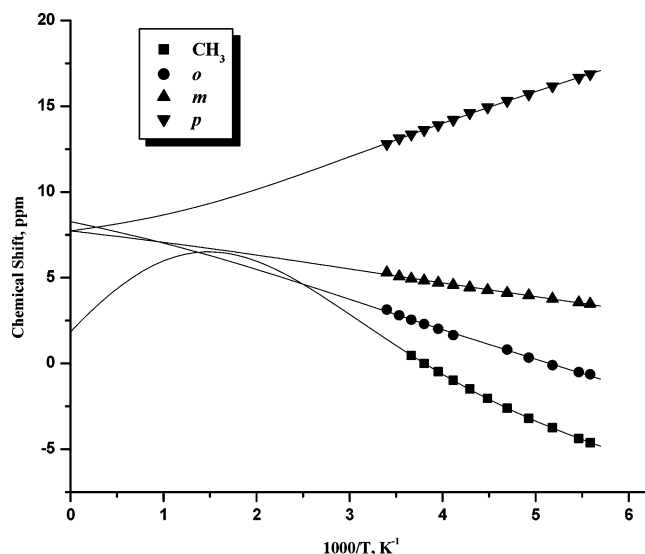

Figure 6. Curie plot of all porphyrin proton resonances in [FeOMTPP-(t-BuNC)$_2$]ClO$_4$, with a 2-level fit[21,22] for a $S = ^3/_2$ excited state lying 700 cm^{-1} above the $S = ^1/_2$ ground state having a $(d_{xz},d_{yz})^4(d_{xy})^1$ electron configuration (the fit did not converge if the excited state was assumed to have $S = ^1/_2$ with the $(d_{xy})^2(d_{xz},d_{yz})^3$ electron configuration). Derived spin densities for ground- and excited-state orbitals, respectively, are as follows: CH$_3$, -0.00220, $+0.01204$; o-H, 0.00326, 0.00211; m-H, -0.00334, -0.00107; and p-H, 0.00155, 0.00122. The negative spin densities at the $meta$-H positions for both ground- and excited-state orbitals are indicative of the presence of positive π spin density at the $meso$-carbons in both cases, while the reason for the negative spin density at the β-CH$_3$ protons is not clear, but is small for the β-pyrrole positions.

dependence using the 2-level temperature-dependent fitting program (TDFw) created by Nikolai V. Shokhirev in this laboratory[22] indicates that, while the ground-state indeed has the $S = ^1/_2$ $(d_{xz},d_{yz})^4(d_{xy})^1$ electron configuration, the excited state, which lies some 700 cm^{-1} higher in energy, does not have the *other* $S = ^1/_2$ electron configuration, $(d_{xy})^2(d_{xz},d_{yz})^3$,[30] but rather has $S = ^3/_2$, with reasonably large spin density at the pyrrole carbons. This large spin density is suggestive of either a $(d_{xz},d_{yz})^3(d_{xy})^1(d_{z^2})^1$ or a $(d_{xy})^2(d_{xz},d_{yz})^2(d_{z^2})^1$ electron configuration for the $S = ^3/_2$ excited state. In fact, as will be discussed in more detail elsewhere,[31] similar analysis of the temperature dependence of the proton shifts [FeOETPP(t-BuNC)$_2$]$^+$ and [FeTC$_6$TPP(t-BuNC)$_2$]$^+$ indicate that they also have thermally-accessible $S = 3/2$ excited states that lies 130 and 880 cm^{-1} higher in energy, respectively. The saddled octaalkyltetraphenylporphyrinate complexes of Fe(III) in several different spin states appear to have a tendency to have $S = ^3/_2$ excited states.[31]

2D ^{1}H NMR experiments (COSY, NOESY, and ROESY) were carried out in the temperature range from 0 to -50 °C and at -90 °C. As can be seen from Table 4, the T_1s of all protons in [FeOMTPP(t-BuNC)$_2$]ClO$_4$ are, in general, relatively short (15−100 ms) and decrease as the temperature is lowered. Short relaxation times are the result of fast molecular motion (inversion) of the OMTPP porphyrin core, as well as ligand exchange, the latter of which mixes in higher spin states of the metal, which have significantly shorter T_1 relaxation times. On the other hand, the T_1 of free t-BuNC increases with decreasing temperature, as expected for a diamagnetic molecule whose T_1 is determined by η/T, where η is the viscosity of the solvent. Because of the short

(27) Ogura, H.; Yatsunyk, L.; Medforth, C. J.; Smith, K. M.; Barkigia, K. M.; Renner, M. W.; Melamed, D.; Walker, F. A. *J. Am. Chem. Soc.* **2001**, *123*, 6564−6578.
(28) Ikeue, T.; Ohgo, Yo.; Yamaguchi, T.; Takahashi, M.; Takeda, M.; Nakamura, M. *Angew. Chem., Int. Ed.* **2001**, *40*, 2617−2620.
(29) Yatsunyk, L. A.; Ogura, H.; Walker, F. A. To be submitted for publication.
(30) The fit does not converge if $S = ^1/_2$ is assumed for the excited state.
(31) Yatsunyk, L. A.; Shokhirev, N. V.; Walker, F. A. To be submitted for publication.
(32) Cheng, R.-J.; Chen, P.-Y.; Gau, P.-R.; Chen, C.-C.; Peng, S.-M. *J. Am. Chem. Soc.* **1997**, *119*, 2563−2569.
(33) Yatsunyk, L. A. Ph.D. Dissertation, University of Arizona, 2003.

Table 4. Chemical Shifts and T_1 Relaxation Times for [FeOMTPP(t-BuNC)$_2$]ClO$_4$ in CD$_2$Cl$_2$ at Two Temperatures

peak	$T = -10°C$		$T = -90°C$		assignment
	shift, ppm	T_1, sec	shift, ppm	T_1, sec	
L	−1.72	0.106(9)	−3.39	0.0037(1)	bound ligand, t-Bu
CH$_3$	0.93	0.0226(1)	−4.37	0.0057(3)	porphyrin methyl
F	1.41	0.160(3)	1.43	0.454(2)	free ligand, t-Bu
o	2.81	0.014(2)	−0.50	0.0010(3)	porphyrin $ortho$-phenyl
p	5.07	0.0988(7)	3.56	0.0178(10)	porphyrin $para$-phenyl
m	13.13	0.0695(2)	16.67	0.0110(2)	porphyrin $meta$-phenyl

relaxation times, any experiments with several pulses and delays, such as DQF−COSY, result in spectra with diminished cross-peak intensity or even cross-peaks being lost. Thus magnitude-mode COSY spectra were used for the peak assignments. It was possible to assign the porphyrin phenyl resonances on the basis of m−p and m−o cross-peaks. The m−o cross-peaks were very weak because the T_1 of the phenyl-*ortho* peak is only 0.014 s at −10° and decreases as the temperature is lowered further.

In both NOESY and ROESY experiments the following cross-peaks were seen: NOE between phenyl m−p at all temperatures, due to proximity of these protons to each other; NOE between phenyl m−o only at 0 and −10 °C; chemical exchange (CE) cross-peaks between bound (L) and free (F) t-Bu signals, indicating fast ligand exchange. Below −50 °C this process becomes too slow on the NMR time scale for the F−L cross-peaks to be observed. Ring inversion cannot be detected in the [FeOMTPP(t-BuNC)$_2$]ClO$_4$ complex because of its high symmetry, which produces chemical and magnetic equivalence for all eight methyl groups.

Proton 1- and 2D NMR studies of [FeTC$_6$TPP(t-BuNC)$_2$]ClO$_4$. NMR experiments for the [FeTC$_6$TPP(t-BuNC)$_2$]ClO$_4$ complex were done in the temperature range from +30 to −90 °C, and two example spectra, at −10 and −80 °C, together with the peak assignments are shown in Figure 7. Unlike the cases of [FeOETPP(t-BuNC)$_2$]ClO$_4$ and [FeOMTPP(t-BuNC)$_2$]ClO$_4$, binding of t-BuNC to TC$_6$TPPFe(III) is much more favorable, and relatively sharp peaks for free and bound ligand t-Bu protons are observed, even at fairly high temperature (see Figure 7, 1D NMR spectrum at −10 °C). Peak assignment was based on COSY results and is presented in Table 5, with the corresponding relaxation times, T_1s. From this table one can see that all protons of [FeTC$_6$TPP(t-BuNC)$_2$]ClO$_4$ have very short T_1 values that decrease upon lowering the temperature. The flexibility of the TC$_6$TPP porphyrin core is the highest in the series of octaalkyltetraphenylporphyrinatoiron(III) complexes of the present study, which results in the shortest relaxation times for the porphyrin protons. For peaks that are close to the paramagnetic center (CH$_2(\alpha)$ and phenyl-*ortho*) the T_1 even at room temperature is on the order of 10 ms. As the temperature decreases, the T_1s become too short for these peaks to be observed even in simple 1D NMR experiments (Figure 7, 1D NMR spectrum at −80 °C). Linear temperature dependences of the chemical shifts of the Curie plot (supplementary Figure S5) were extrapolated to infinite temperature ($T^{-1} = 0$), and the chemical shifts obtained were compared to those for the free porphyrin, H$_2$TC$_6$TPP. For all peaks except CH$_2(\alpha)$ the chemical shifts at infinite
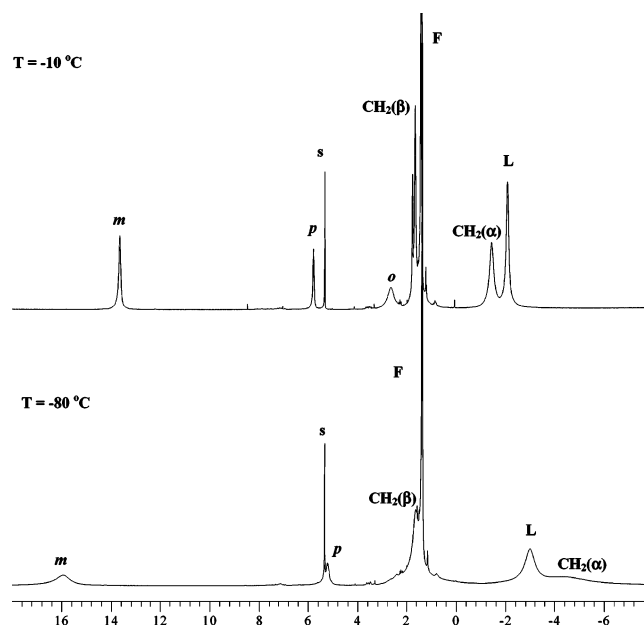

Figure 7. ^{1}H NMR spectra of [FeTC$_6$TPP(t-BuNC)$_2$]ClO$_4$ in CD$_2$Cl$_2$, recorded at −10 and −80 °C, together with peak assignments: o, m, p, phenyl resonances; F and L, free and ligated t-Bu protons; CH$_2(\alpha)$ and CH$_2(\beta)$, methylene protons in α and β positions with respect to the pyrrole β-Cs.

temperature match fairly well with the diamagnetic shifts. However, for CH$_2(\alpha)$ the extrapolated shift was much higher than the diamagnetic shift (6.99 vs 2.33 ppm), suggesting the likelihood of a $S = {}^3/_2$ excited state in this case as well as discussed further below.

NOESY and ROESY experiments (the latter made possible by the fact that the spectral window is narrow enough for ROESY spin-lock) were used to supplement and verify the assignments from COSY data and to assign free and bound ligand t-Bu resonances. Both techniques were used only down to −70 °C, because at lower temperatures all peaks had extremely short T_1s and were not observed (or were very broad) in the 2D spectra. From NOESY and ROESY experiments we have learned that ligand exchange is detectable in solutions of [FeTC$_6$TPP(t-BuNC)$_2$]ClO$_4$ only above −20 °C, which is a much higher temperature than that for the OMTPP or OETPP complexes. On the other hand, ring inversion is very fast on the NMR time scale at any temperature. This is not surprising, as it has been shown elsewhere[13,29] that the flexibility of the porphyrin core in TC$_6$TPP is very high compared to that in either OMTPP or OETPP. And also from that work, whereas ring inversion in (TC$_6$TPP)FeCl is close to the detection limit of NMR spectroscopy, based on the fact that the free energy of activation, $\Delta G^{\ddagger}_{298}$, in (OETPP)FeCl is twice as high as

Table 5. Chemical Shifts and T_1 Relaxation Times for [FeTC$_6$TPP(t-BuNC)$_2$]ClO$_4$ in CD$_2$Cl$_2$ at Two Temperatures

	$T = -10°C$		$T = -80°C$		
peak	shift, ppm	T_1, sec	shift, ppm	T_1, sec	assignment
L	−2.09	0.0134(3)	−2.99	0.0030(1)	bound ligand, t-Bu
CH$_2$(α)	−1.45	0.0083(1)	−4.35	0.0017(2)	methylene (α)
F	1.41	0.739(5)	1.49	0.595(2)	free ligand, t-Bu
CH$_2$(β)	1.66	0.0264(3)	1.63	<0.0118(3)^a	methylene (β)
o	2.65	0.0042(2)	0.80^b	too short	porphyrin $ortho$-phenyl
p	5.78	0.0600(4)	5.21	0.0128(1)	porphyrin $para$-phenyl
m	13.65	0.0368(1)	15.94	0.0092(1)	porphyrin $meta$-phenyl

^{a} This value was obtained at −50 °C. At lower temperatures CH$_2$(β) peak overlaps with some impurities which preclude accurate measurement of T_1. Considering T_1 decreases upon lowering temperature, its value at −80 °C should be smaller than that presented. ^{b} Calculated from the Curie plot (Figure S5) by extrapolating the line for the porphyrin $ortho$-phenyl to −80 °C, where this peak is too broad to be observed.

$\Delta G^{\ddagger}_{298}$ for [FeOETPP(t-BuNC)$_2$]ClO$_4$ (66(4) vs 36(1) kJ mol^{-1}),[29] a much faster rate of ring inversion, well beyond the detection limit of NMR spectroscopy, is predicted for [FeTC$_6$TPP(t-BuNC)$_2$]ClO$_4$.

At high temperatures the following NOE cross-peaks can be observed in NOESY and ROESY spectra: $m − p$, $m − $L($t$-Bu), and CH$_2$($\alpha$) − CH$_2$($\beta$), which are consistent with our assignment from the COSY spectra. NOE cross-peaks between phenyl-$meta$ and L(t-Bu) are interesting because they provide information about the orientation of the phenyl rings with respect to the porphyrin core: as commonly found in saddled porphyrins, the phenyl rings rotate into the porphyrin plane to minimize unfavorable contacts with the substituents on the β-pyrrole carbons. In general, the orientation of the phenyl ring correlates with the degree of saddled distortion in the molecule: a steeper saddled distortion results in a more acute phenyl dihedral angle. On the other hand, in ruffled porphyrins, the phenyl dihedral angles are much closer to perpendicular to the porphyrin plane, bringing phenyl-$meta$ close to the methyl groups of the t-BuNC ligand. Thus, from the NMR spectra (NOEs) some conclusions can be drawn about the average geometry of the porphyrin core in [FeTC$_6$TPP(t-BuNC)$_2$]ClO$_4$: it is partially ruffled, resulting in the phenyl-$m − $L($t$-Bu) NOE cross-peaks in the 2D spectra, and much less distorted from planarity as compared to [FeOETPP(t-BuNC)$_2$]ClO$_4$ and [FeOMTPP(t-BuNC)$_2$]-ClO$_4$, because the rate of ring inversion is very fast on the NMR time scale. The NMR conclusions are supported by structural data for (OETPP)FeCl, (OMTPP)FeCl,[32] and (TC$_6$TPP)FeCl.[33] The latter complex is the most planar and the most ruffled of the three. The same can be said about the geometry of [FeOETPP(1-MeIm)$_2$]Cl, [FeOMTPP(1-MeIm)$_2$]Cl, and [FeTC$_6$TPP(1-MeIm)$_2$]ClO$_4$.[13]

NMR Spectra and Spin State of S$_4$-Saddled Porphyrins. In solution NMR studies of bis-(t-BuNC) iron(III) complexes of OETPP, OMTPP, and TC$_6$TPP, two chemical exchange processes have been detected: ligand exchange and ring inversion. The first process becomes undetectable on the NMR time scale at −70, −50, and −20 °C for OETPP, OMTPP, and TC$_6$TPP, respectively, indicating that the binding abilities of the porphyrins of this study to t-BuNC increase in the following order OETPP < OMTPP < TC$_6$TPP. Ring inversion for [FeOETPP(t-BuNC)$_2$]ClO$_4$ was studied in great detail, and the results are presented elsewhere.[29] In general, ring inversion in nonplanar porphyrins correlates directly with the planarity of their cores, and

therefore, the rate of ring inversion decreases in the order TC$_6$TPP > OMTPP > OETPP. It is also interesting to note that the chemical shift of the methyl protons of the bound ligand, t-BuNC, decreases in the same order (−2.99 at −80 °C, −3.39, −4.41 ppm at −90 °C, for TC$_6$TPP, OMTPP, and OETPP, respectively). This trend is in line with the fact that the nonplanar distortion of the porphyrin ring increases in the order TC$_6$TPP < OMTPP < OETPP, and the OETPP molecule will thus have ring currents that extend much higher on the axial ligand than will the relatively planar TC$_6$TPP molecule. That this is a ring current effect is suggested by the fact that (1) the dipolar contributions to the isotropic shifts are very small and identical for the three complexes because the very small g-anisotropy and nearly identical g-values of all three, and (2) there can be no π contact shift transmitted from the d$_{xy}$ unpaired electron of low-spin Fe(III) to the p$_\pi$ orbitals of t-BuNC because of the orthogonality of the orbitals involved. Although there could be differences in σ contact shifts or spin polarization for the three, these are difficult to evaluate and the small differences in methyl shifts noted above are certainly consistent with a difference in the height of the ring current felt by the axial ligands in the three complexes.

For the novel (d$_{xz}$,d$_{yz}$)^4(d$_{xy}$)^1 ground state, the d$_\pi$ orbitals of Fe(III) are filled, but the d$_{xy}$ unpaired electron can engage in spin delocalization to the porphyrinate ring if it is ruffled, and such ruffling is quite extreme in many of the reported complexes.[6,7,9] In line with this, the pyrrole-H chemical shifts for the bis-(t-BuNC)[3] and bis-(4-CNPy)[6] complexes of TPPFe(III) and for the bis-(2,6-XylylNC) complex of p-TPPFe(III)[9] are fairly close to their diamagnetic values (with allowances for the differing ring-current shifts of differently distorted porphyrinate rings), whereas the $meso$-phenyl-H shift differences, $\delta_m − \delta_p$ and $\delta_m − \delta_o$, are both large and positive (+12 to +19 ppm at ambient temperatures),[6,7,9,34] indicating large positive spin density at the $meso$-Cs. In the saddled bis-(t-BuNC) complexes of OETPP, OMTPP, and TC$_6$TPP a similar trend is observed: the $meso$-phenyl-H chemical shift differences, $\delta_m − \delta_p$ and $\delta_m − \delta_o$, are both large and positive (+5 to +11 at −20 °C), but significantly smaller (∼50%) than the same values in ruffled porphyrins (Table 6). Spin delocalization to the $meso$-carbons is reduced in saddled porphyrins, where the mechanism of stabilization of the (d$_{xz}$,d$_{yz}$)^4(d$_{xy}$)^1 ground state by porphyrin $3a_{2u}(\pi) \rightarrow$

(34) Walker, F. A. *Inorg. Chem.* **2003**, *42*, 4526−4544.

Table 6. Chemical Shifts for Selected Resonances in Complexes with $(d_{xz},d_{yz})^4(d_{xy})^1$ Ground State

porphyrin	T, K	δ_{pyrr} [a]	δ_m	δ_p	δ_o	$\delta_m-\delta_p$	$\delta_m-\delta_o$	sum $(\delta_m-\delta_p)+(\delta_m-\delta_o)$
[FeOETPP(t-BuNC)$_2$]$^+$	253	+8.33	+11.41	+6.30	+5.54	+5.11	+5.87	10.98
[FeOMTPP(t-BuNC)$_2$]$^+$	263	+0.94	+13.13	+5.07	+2.81	+8.06	+10.32	18.38
[FeTC$_6$TPP(t-BuNC)$_2$]$^+$	263	−1.45	+13.65	+5.78	+2.65	+7.87	+11.00	18.87
[FeTPP(t-BuNC)$_2$]$^+$ [b]	298	+9.7	+13.8	+3.2	+1.0	+10.6	+12.8	23.4
[Fe(p-TTP)(2,6-XylylNC)$_2$]$^+$ [e]	297	+10.7	+16.5	+2.4 [c]	−3.4	+(lg) [d]	+19.9	−

[a] δ_{pyrr}: CH$_3$ group for OMTPP, CH$_2$(outer) for OETPP, and CH$_2(\alpha)$ for TC$_6$TPP. [b] Results taken from ref 33. [c] Methyl-H shift. [d] Expected positive and large difference. [e] Results taken from ref 9.

iron d_{xy} delocalization is expected to be generally reduced. Small spin delocalization to the porphyrin β-positions in the bis-(t-BuNC) octaalkyltetraphenylporphyrin complexes is reflected in the diamagnetic values of the chemical shifts of methyl (OMTPP) and methylene (OETPP and TC$_6$TPP) resonances (see Table 6).

The EPR g-values for [FeOETPP(t-BuNC)$_2$]ClO$_4$, [FeOMTPP(t-BuNC)$_2$]ClO$_4$ and [FeTC$_6$TPP(t-BuNC)$_2$]ClO$_4$ are very similar to each other and to the corresponding values for [FeOEP(t-BuNC)$_2$]ClO$_4$,[7] [FeTPP(t-BuNC)$_2$]ClO$_4$,[7] and [FeTTP(2,6-XylylNC)$_2$]ClO$_4$,[9] whose structures are all known to be strongly ruffled,[7,9] thus suggesting that the electronic ground state of iron(III) is the same for all of these complexes, i.e., $(d_{xz},d_{yz})^4(d_{xy})^1$, as discussed above. However, although the phenyl proton chemical shifts are also similar in pattern, they are much smaller in magnitude than those of [FeTPP(t-BuNC)$_2$]ClO$_4$[3] and [FeTTP(2,6-XylylNC)$_2$]-ClO$_4$.[9] This suggests that all three complexes of this study have comparably pure $(d_{xz},d_{yz})^4(d_{xy})^1$ electronic states, but with less spin delocalization from the metal to the porphyrinate ring. The smaller positive values of the *meso*-phenyl chemical shift differences, $\delta_m - \delta_p$ and $\delta_m - \delta_o$ (Table 6), as well as ^{13}C results[18] for [FeOETPP(t-BuNC)$_2$]ClO$_4$, suggest that the spin densities at the *meso*-carbons are smaller for this complex than for those of the analogous OMTPP and TC$_6$TPP complexes, and that all three are smaller than those of [FeTPP(t-BuNC)$_2$]ClO$_4$.[3] Because of somewhat uneven shift differences, $\delta_m - \delta_p$ and $\delta_m - \delta_o$, for the complexes of this study, perhaps the best guide is the sum of these two shift differences, given in the last column of Table 6. By this evaluation, the contribution of the $(d_{xz},d_{yz})^4(d_{xy})^1$ state to spin delocalization to the porphyrinate core decreases in the order TPP > TC$_6$TPP ≈ OMTPP ≫ OETPP with the three dodecasubstituted iron porphyrinates under study having 81, 79, and 47% as much spin density (as compared to the TPP analogue, 100%), respectively, at the *meso*-carbons, as sensed by the ^{1}H shift differences of the phenyl protons (Table 6). This order is in accord with the structural results, which indicate a purely saddled conformation for [FeOMTPP(t-BuNC)$_2$]ClO$_4$, and by inference for [FeOETPP-(t-BuNC)$_2$]ClO$_4$, although with larger deviations from the mean plane of the porphyrin ring, and an inferred more-or-less equal mixture of saddled and ruffled geometry of [FeTC$_6$TPP(t-BuNC)$_2$]ClO$_4$ (based on the structures of (TC$_6$TPP)FeCl[33] and [FeTC$_6$TPP(1-MeIm)$_2$]Cl),[13] as compared to the ruffled geometry of [FeTPP(t-BuNC)$_2$]ClO$_4$.[7] On this basis the above order might be TPP > TC$_6$TPP > OMTPP ≫ OETPP, with the only difference being the degree of similarity in the position of TC$_6$TPP and OMTPP. In any

case, from these studies it is apparent that the geometry of the porphyrin core is important, but it is not the crucial factor in defining the electronic ground state of iron(III) porphyrinate complexes.

Conclusions

Two crystal structures of [FeOMTPP(t-BuNC)$_2$]ClO$_4$ were obtained with purely saddled porphyrin cores and asymmetrical environments around Fe(III). To our knowledge this is the first example of a porphyrin complex with a purely saddled conformation that stabilizes the $(d_{xz},d_{yz})^4(d_{xy})^1$ ground state. Usually, ruffled geometry is required because twisting of the pyrrole rings creates an xy component for the porphyrin nitrogen p$_z$ orbitals and, therefore, proper symmetry for interaction of the porphyrin a_{2u} orbital with an unpaired electron in the d_{xy} orbital of Fe(III).[6] Therefore, all complexes with $(d_{xz},d_{yz})^4(d_{xy})^1$ ground state for which structures have been reported previous to this work have adopted ruffled geometries.[7,9]

On the basis of NMR and EPR spectroscopic results, the following points can be made. (i) The ground state of bis-(t-BuNC) complexes of OETPP, OMTPP, and TC$_6$TPP are represented mainly (99.1−99.4%) as a $(d_{xz},d_{yz})^4(d_{xy})^1$ electron configuration, with an excited-state lying 700 cm^{-1} to higher energy for the OMTPP complex and at lower and higher energies, respectively, for the OETPP and TC$_6$TPP complexes. (ii) Although EPR spectroscopy is an excellent technique for determination of metalloporphyrin ground state, it is limited to low temperatures only, whereas ^{1}H chemical shifts give a clear indication of the ground state of the porphyrin complex at ambient temperatures. (iii) The $(d_{xz},d_{yz})^4(d_{xy})^1$ ground state, which has large spin delocalization to the porphyrin *meso*-positions and small delocalization to the β-Cs, is characterized by large and positive *meso*-phenyl-H shift differences, $\delta_m - \delta_o$ and $\delta_m - \delta_p$, and close to diamagnetic shifts of groups (CH$_3$ or CH$_2$) directly attached to β-Cs. (iv) The flexibility of the porphyrin core decreases with increasing nonplanar distortion in the order TC$_6$TPP > OMTPP > OETPP, and in the same order the binding ability to t-BuNC ligands decreases. (v) Finally, and most important, we conclude that a *ruffled geometry stabilizes the $(d_{xz},d_{yz})^4(d_{xy})^1$ ground state but is not necessary for its existence*. Therefore, the ground state of iron(III) porphyrinate complexes is defined mainly by the number and type of axial ligands, and delocalization of spin density to the porphyrin ligand is a relatively minor contribution to the electronic ground state.

Supporting Information Available: Details of the structure determinations (pdf): Figure S1, crystal packing of dodecane molecules in [FeOETPP(t-BuNC)$_2$]ClO$_4$; Figure S2, linear display of the deviation of the macrocycle atoms from the mean porphyrin plane for A and B; Figures S3 and S5, Curie plots of proton resonances in [FeOETPP(t-BuNC)$_2$]ClO$_4$ and [FeTC$_6$TPP(t-BuNC)$_2$]-ClO$_4$, respectively; Figure S4, ^{1}H NMR spectra of [FeOMTPP(t-BuNC)$_2$]ClO$_4$; Tables S1−S5, atomic coordinates and equivalent isotropic displacement parameters; bond lengths and angles; anisotropic displacement parameters; hydrogen coordinates and isotropic displacement parameters; torsion angles for [FeOMTPP(t-BuNC)$_2$]-ClO$_4$, molecule A; Tables S6−S10, the same for molecule B. Crystallographic information files for the complexes (cif). This material is available free of charge via the Internet at http://pubs.acs.org.

IC035242P